

UCLA

UCLA Previously Published Works

Title

Ion ejection from a permanent-magnet mini-helicon thruster

Permalink

<https://escholarship.org/uc/item/75j607q1>

Journal

Physics of Plasmas, 21(9)

ISSN

1070-664X

Author

Chen, Francis F

Publication Date

2014-09-01

DOI

10.1063/1.4896238

Peer reviewed

Ion ejection from a permanent-magnet mini-helicon thruster

Francis F. Chen

Electrical Engineering Department, University of California, Los Angeles 90095-1594, USA

(Received 18 July 2014; accepted 8 September 2014; published online 26 September 2014)

A small helicon source, 5 cm in diameter and 5 cm long, using a permanent magnet (PM) to create the DC magnetic field \mathbf{B} , is investigated for its possible use as an ion spacecraft thruster. Such ambipolar thrusters do not require a separate electron source for neutralization. The discharge is placed in the far-field of the annular PM, where \mathbf{B} is fairly uniform. The plasma is ejected into a large chamber, where the ion energy distribution is measured with a retarding-field energy analyzer. The resulting specific impulse is lower than that of Hall thrusters but can easily be increased to relevant values by applying to the endplate of the discharge a small voltage relative to spacecraft ground. © 2014 AIP Publishing LLC. [<http://dx.doi.org/10.1063/1.4896238>]

I. INTRODUCTION

Spacecraft thrusters now in orbit are mostly of two types: electrostatic ion thrusters and Hall thrusters. These are much more efficient than the chemical or MHD thrusters used in early days of space exploration. Ion thrusters create a plasma with a voltage applied between a thermionic cathode and an anode grid. The ions passing through that grid are accelerated to high velocity by a second grid and form the ion beam that pushes the spacecraft forward by momentum conservation. Xenon is normally used because of its inertness and high mass. A source of cool electrons is needed to neutralize the space charge of the ion beam. Hall thrusters produce a denser plasma by holding the electrons back with a B-field as the ions are accelerated by an electrostatic voltage. An electron source for neutralization is also needed here.

One measure of the effectiveness of a thruster is the specific impulse, I_{sp} , defined as

$$I_{sp} \equiv \frac{v_{ex} \text{ m/s}}{g \text{ m/s}^2} \text{ s}, \quad (1)$$

where v_{ex} is the ion exhaust velocity. The speed which the spacecraft can reach depends on the amount of xenon available for ejection. This consideration of mass is outside the scope of this paper but can be found in standard references.¹ Helicons can produce higher plasma density n than most other discharges at the same power and therefore have been suggested for use in thrusters. Since the plasma is not fully ionized, neutral atoms entrained by the ions will also be ejected, thus increasing the effective I_{sp} . Thus, only a lower limit to I_{sp} can be found from our measurements. A large literature has arisen on helicon thrusters, and reviews of this subject have been published by Charles.^{2,3} Helicons require a DC magnetic field, and almost all experiments so far have produced the B-field with heavy copper coils driven by a DC power supply. By designing a small but dense helicon source using permanent magnets, we have greatly reduced the size and weight of the thruster. In this paper, we show how the design was made and how I_{sp} was measured using an ion energy analyzer. We have increased I_{sp} by applying an electric potential, as it is done in Hall thrusters.

II. DESIGN OF THE HELICON SOURCE

A. Tube design

Among plasma discharges, helicons are probably the most complicated, since they involve magnetic fields, neutral collisions, fancy antennas, and RF coupling mechanisms that include parametric instabilities. Fortunately, the design of an experiment has been facilitated by the program HELIC written by Arnush.⁴ After setting the RF frequency, the gas, and the discharge dimensions, the most useful plot that one can obtain is that of $R(n, B)$, where R is the plasma resistance, proportional to the RF energy absorption. A typical result is shown in Fig. 1. To overcome circuit resistance, R should be at least 1Ω . Stable operation occurs on the downward slope of each curve, where a drop in n leads to higher absorption, and vice versa. $R(n, B)$ plots for various discharge tube radii a and height h led to the tube shown in Fig. 2. The top plate (endplate) has to be conducting (aluminum), so that the reflected back-wave interferes constructively with the downward forward wave when h has the proper value. The antenna is placed as close as possible to the exit to avoid losing plasma to the sidewalls. The “skirt” on the bottom is to minimize induced currents in the flange on which the tube is mounted.

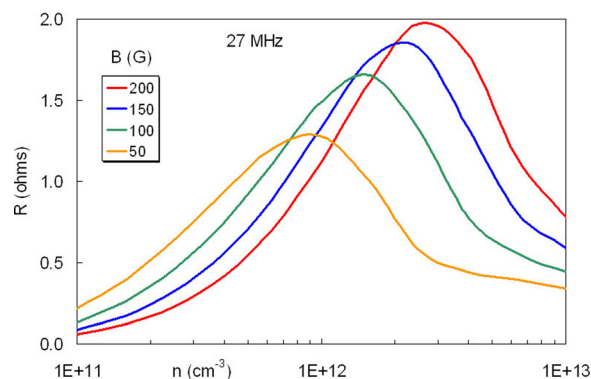


FIG. 1. A HELIC plot of plasma resistance R vs. n and B for the tube dimensions in Fig. 2.

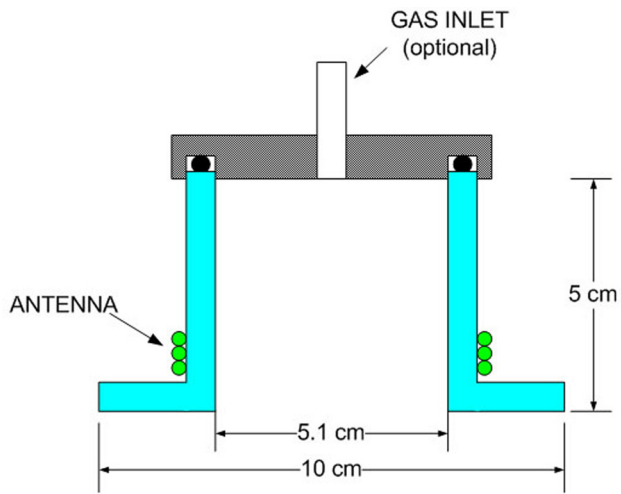


FIG. 2. Final design of the discharge tube. The antenna has three turns for 13 MHz and one turn for 27 MHz.

B. Magnet design

Annular magnets polarized vertically have a strong field inside the hole, but plasma produced there will flow sideways along field lines instead of downward. The discharge is therefore placed below the stagnation point, where the B-field is weaker but is quite uniform and extends to infinity. The bottom rectangle in Fig. 3 shows a sample position of the discharge tube. The B-field can be varied by moving the magnet vertically relative to the tube. Thus, the common notion that PMs cannot provide variable B-fields is not a real restriction. The magnet shown in Fig. 3 is a neodymium (NdFeB) magnet of 3 in. (7.6 cm) inner and 5 in (12.7 cm) outer diameters and is 1 in. (2.54 cm) thick. Previous experiments with this magnet showed that its strong B-field was not necessary, and it has been replaced with a commercially

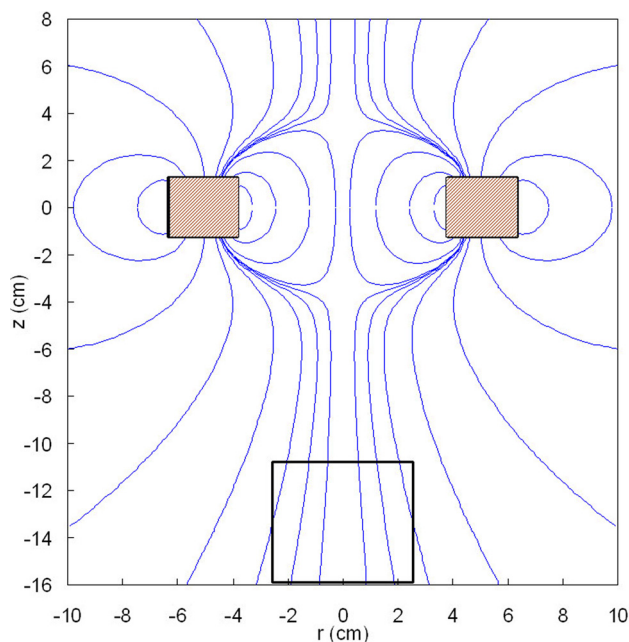


FIG. 3. Field lines of an annular permanent magnet and possible position of the discharge tube.

available Nd magnet of 2 in. ID and 4 in. OD, $\frac{1}{2}$ in thick. A picture of the discharge with this smaller magnet is shown in Fig. 4.

Permanent magnets have also been used for helicon thrusters by Takahashi *et al.*^{5,6} In a much larger experiment, the magnets are linear rather than the annular ones used here in their remote, reverse fields. Takahashi measured the thrust directly by suspending the entire magnet + discharge system and measuring its displacement when the RF is turned on.

III. EXPERIMENTAL SETUP

A. Plasma chamber

The helicon source is mounted on the large chamber shown in Fig. 5. The retarding-field energy analyzer (RFEA) is mounted on a vertical shaft that can position it at variable distances z below the source. Three ports on the side permit the insertion of probes for radial measurements at three z 's. Unless otherwise specified, "standard conditions" are with the large magnet of Fig. 3, a pressure of 15 mTorr of argon, and 400 W of 27.12 MHz RF power.

B. Ion analyzer

The RFEA is the SEMionTM made by Impedans, Ltd.^{7,8} The system is designed to work in a strong RF environment. The sensor is shown in Fig. 6. Its aluminum case is approximately 10 cm in diameter and 1 cm thick, covered with aluminum oxide. Its capacitance to ground is small, so that the

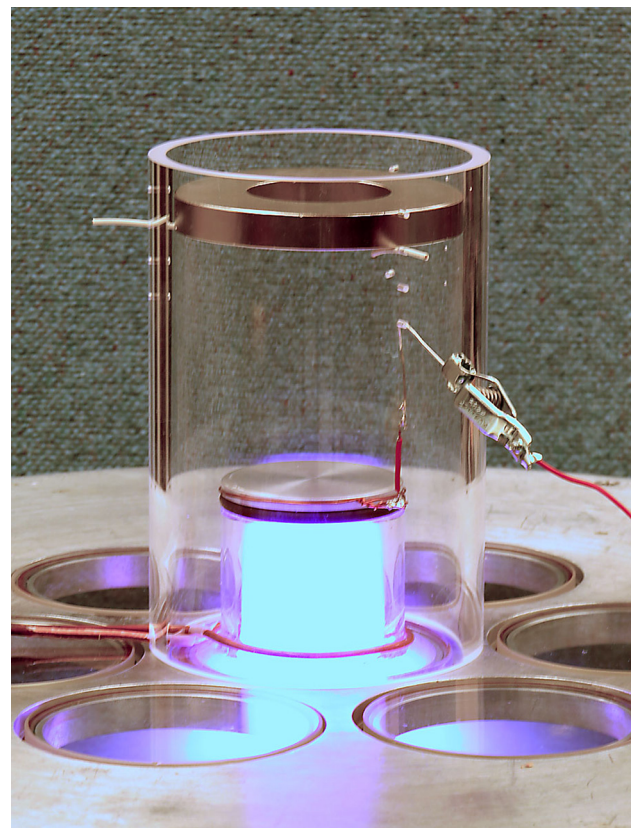


FIG. 4. Photo of the helicon discharge with a commercial Nd magnet at its optimum height. The top plate (endplate) of the discharge is aluminum and can be grounded or biased with a battery relative to machine ground.

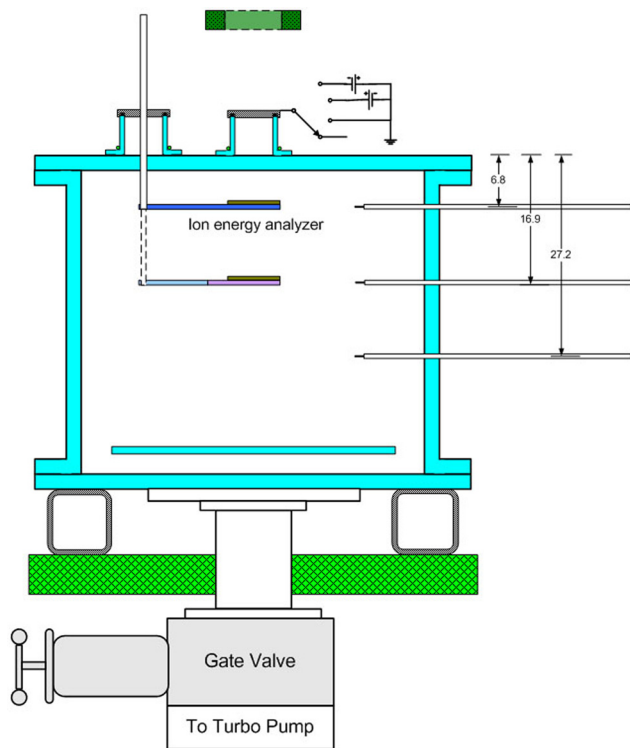


FIG. 5. Diagram of the experimental chamber. The magnet is the one shown in Fig. 3; its support is not shown. The top plate of the discharge tube is normally grounded but can be biased with a battery as shown. Dimensions are in cm.

entire grid assembly, shown in Fig. 7, follows the RF at the local floating potential. The orifices are $800\ \mu\text{m}$ in diameter, and grid G_0 has $20\ \mu\text{m}$ holes, smaller than the local Debye length. The grid G_1 repels electrons; G_2 provides the swept retarding voltage on the ions; and C is the ion collector. The insulated cable carries the voltages to a filter box, which removes most of the RF and provides DC voltages through a vacuum seal to the control unit. The latter displays $I(V)$ and differentiates it to show the ion distribution. The DC voltage of G_0 was carefully measured with an oscilloscope probe to obtain the floating potential to relate the RFIDs to machine ground.

C. Langmuir probes

The probe tips are of 5-mil (0.127 mm) diameter tungsten, 1 cm long. The $I-V$ curves are obtained with Hiden's ESPTM hardware and analyzed with the author's own software. The probe results verified that the plasmas in this

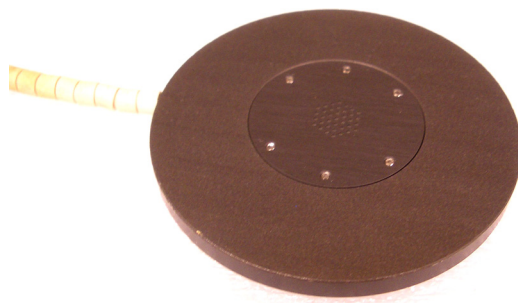


FIG. 6. View of the RFEA from the top.

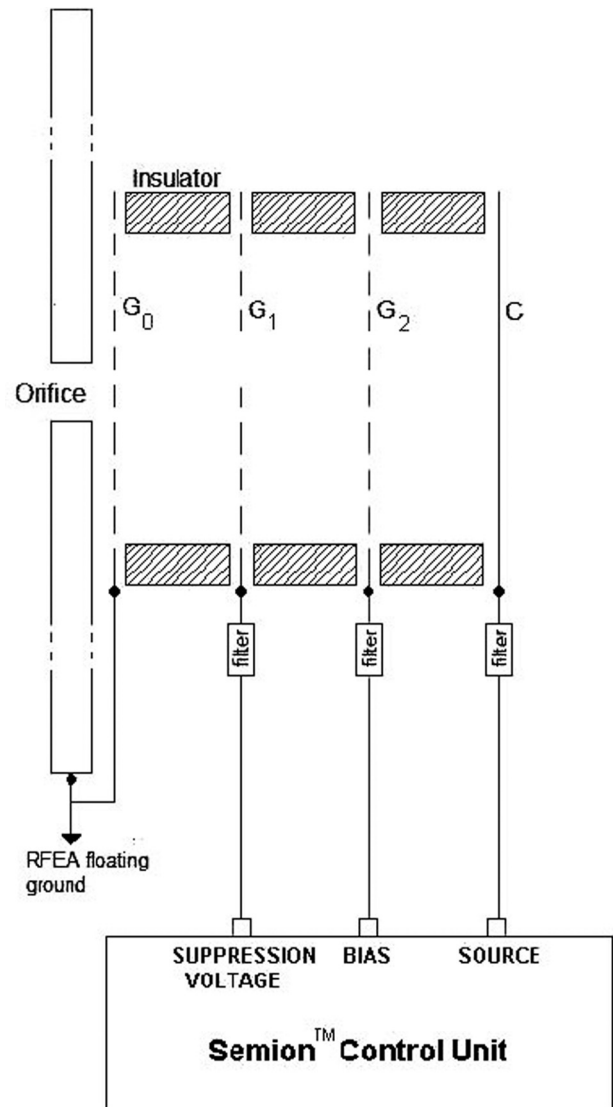


FIG. 7. Diagram of the RFEA.

experiment are the same as those generated in previous years and published previously.⁹ However, when the RFEA sensor is close to the discharge tube, where there is no probe, it forms an endplate for the discharge and under normal circumstances would change the helicon into a shorter discharge. In this case, the RFEA is a floating, so it should not affect the discharge as much as a grounded endplate. To check this, we swung the sensor away from under the tube and checked the RF matching. Only a small change in the tuning was needed.

IV. MEASUREMENTS

The retarding-field ion distributions (RFIDs) obtained are summarized in Fig. 8. The voltages set by the sensor are relative to the floating potential, and these have been converted to voltage relative to ground by subtracting the floating potential. The voltage then represents the ion energy in eV. This process yields negative voltages, which are meaningless, since ion traveling upwards toward the back of the sensor cannot be collected. The negative voltages arise from

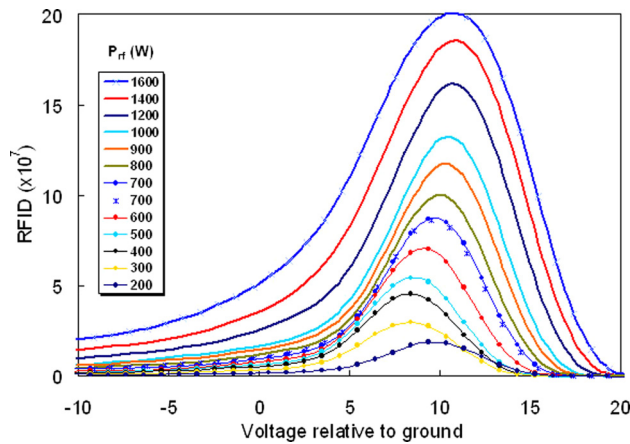


FIG. 8. Ion energy distributions at Port 2 with the large magnet.

the heavy filtering done by the filter unit should be neglected. The RF oscillations in floating potential can be as large as ± 60 V. The sensor is set at Port 2, 16.9 cm below the tube, as seen in Fig. 5. Since the ion-neutral mean free path 15 mTorr of argon pressure is approximately 1 cm, the ion velocities in Fig. 8 are lower than their exit velocities from the source. Unfortunately, the sensor cannot be placed at Port 1 because it is overheated there. Note that the ion velocity increases very little with RF power, a consequence of the fact that KT_e does not change much with power. At 200 W in Fig. 8, the helicon may have gone into a different mode.

The change of RFIDs with distance from the source is shown in Fig. 9 for $P_{rf} = 400$ W. The ions slow down from neutral collisions and lose density due to diffusion, as expected.

To calculate the specific impulse, one should plot the data of Fig. 8 against ion velocity and average over velocity, since I_{sp} is proportional to velocity. However, since filtering has extended the curves into negative velocities, this would not yield accurate results. The curves are fairly symmetric, and it is sufficient to measure only the voltages (i.e., ion energies) at their peaks. Inserting these values into Eq. (1) yields the lower curve for I_{sp} in Fig. 10. This raw value of I_{sp} is too low to be useful, but it can be increased by adding a

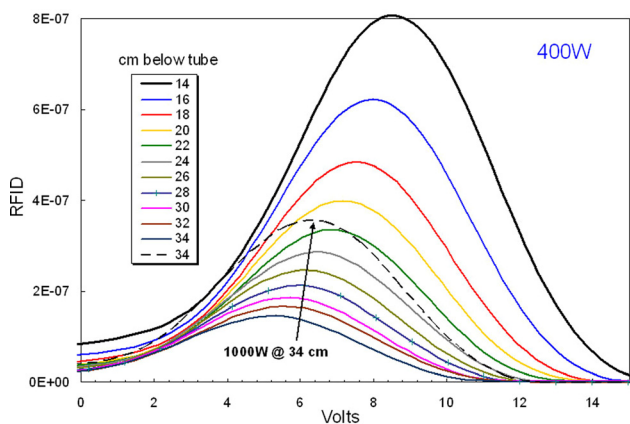


FIG. 9. Z-scan of ion distributions under standard conditions using the small magnet of Fig. 4. The curves are in the order of the legend. The power dependence is illustrated by the dashed curve (1000 W), compared with the bottom curve (400 W).

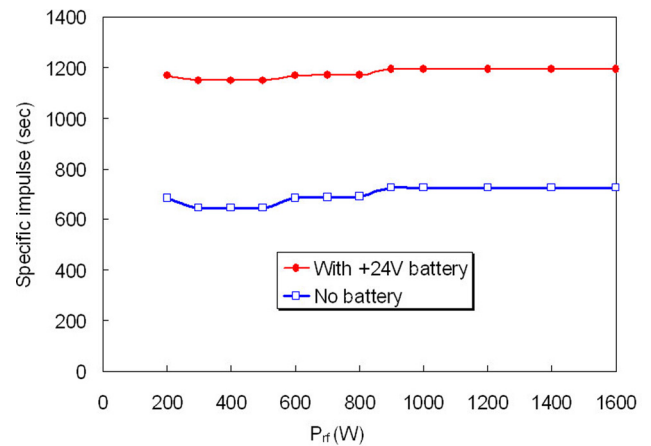


FIG. 10. Specific impulse from a PM helicon thruster at 15 mTorr: intrinsic (\square) and with +24 V bias (\bullet).

bias to the endplate of the helicon source. Because of the severe RF environment near the helicon discharge, an electronic power supply cannot be used. We have used small Pb-acid (car) batteries to apply the bias. Applying +24 V to the endplate with two 12 V batteries in series, we obtained the I_{sp} shown by the top curve in Fig. 10. The value of 1200 there is comparable to what is currently obtained in existing Hall thrusters. For instance, a geostationary satellite operating at 200 V has a v_{ex} of ~ 15 km/s, giving $I_{sp} \sim 1500$ s.¹⁰ This can be achieved with much lower voltage in helicon thrusters.

To show the presence of a strong ion beam even in the absence of a battery, the RFIDs were measured with the sensor facing down, away from the source. The up-down asymmetry is shown in Fig. 11. The source fills the large chamber with plasma, and the backflow due to collisions is measured when the sensor is reversed. In the UP position, the RFID amplitude increases by only about 10% when a +24 V bias is applied to the endplate, indicating that plasma density is not greatly affected by the bias.

At the much lower pressures encountered in space, the ions are not slowed down by collisions as in the above data, and the I_{sp} 's are much higher. Figure 12 shows the RFIDs vs. pressure. The ion density goes down but the energy increases with pressure. For ions of order 2 eV (accelerated by E-fields

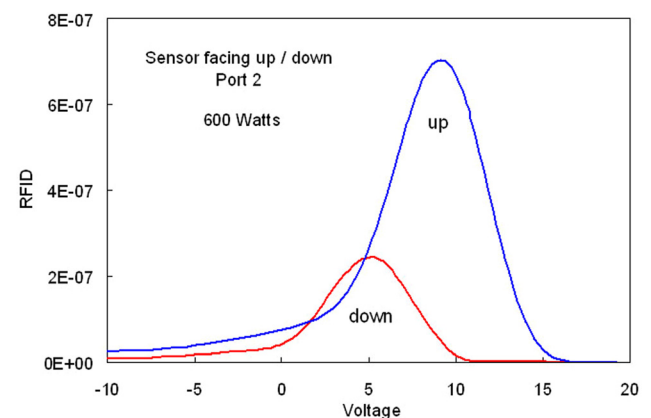


FIG. 11. Ion distributions with the sensor facing the source (up) or away from it (down).

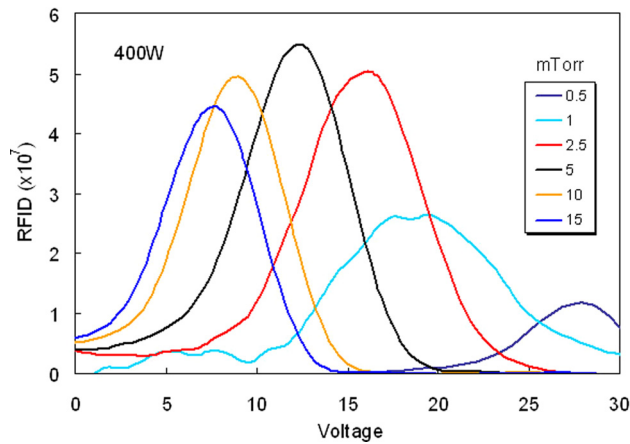


FIG. 12. Ion distributions at 400 W vs. pressure. The legend corresponds to curves reading from left to right.

scaled to KT_e), the ion-neutral mean free path increases from ~ 1 cm at 15 mTorr to ~ 17 cm at 1 mTorr. With the RFID sensor 16.9 cm (Port 2) downstream, the ions reach the sensor directly at 0.5 mTorr, but must diffuse to the sensor at 15 mTorr. At 0.5 mTorr, the peak is at 28 eV, which corresponds to an I_{sp} of 1182 s. Thus, the intrinsic impulse of a PM helicon, before addition of any DC voltage, is already high enough to be useful. The data at higher pressures greatly underestimates I_{sp} , since the ion flux reaching the sensor is diminished by collisions.

V. SUMMARY

Helicon thrusters have drawn attention from the spacecraft community because of their large intrinsic thrust and the circumvention of electron neutralizers. The use of simple

annular permanent magnets greatly reduces the size and weight of the helicon device. Since B-fields of only 30–60 G (3–6 mTorr) are needed, neodymium magnets are not necessary; more stable, weaker magnets, such as SmCo, can be used. The helicon can be driven by a small 200–400 W RF power supply and its matching network. The ions streaming from the source have an intrinsic specific impulse of about 700 s. This can be increased indefinitely by biasing the end-plate of the helicon discharge positively, drawing only milliamperes of current. A bias of only 50 V would bring I_{sp} up to that of Hall-effect thrusters.

ACKNOWLEDGMENTS

This work was made possible by the loan of the SEMion ion analyzer by David Gahan of Impedans, Ltd., of Ireland. We gratefully acknowledge Gahan's help with proper operation of the equipment and interpretation of the results in almost daily communications. We also thank the referee for valuable suggestions used in this version of the paper.

¹D. M. Goebel and I. Katz, *Fundamentals of Electric Propulsion* (John Wiley and Sons, Hoboken, NJ, 2008).

²C. Charles, *Plasma Sources Sci. Technol.* **16**, R1 (2007).

³C. Charles, *J. Phys. D: Appl. Phys.* **42**, 163001 (2009).

⁴D. Arnush, *Phys. Plasmas* **7**, 3042 (2000).

⁵K. Takahashi, T. Lafleur, C. Charles, P. Alexander, R. W. Boswell, M. Perren, R. Laine, S. Pottenter, V. Lappas, T. Harle, and D. Lamprou, *Appl. Phys. Lett.* **98**, 141503 (2011).

⁶K. Takahashi, C. Charles, R. Boswell, and A. Ando, *J. Phys. D: Appl. Phys.* **46**, 352001 (2013).

⁷<http://www.impedans.com/semion-single-sensor>.

⁸C. Hayden, D. Gahan, and M. B. Hopkins, *Plasma Sources Sci. Technol.* **18**, 025018 (2009).

⁹F. F. Chen, *Phys. Plasmas* **19**, 093509 (2012).

¹⁰E. Ahedo, *Plasma Phys. Control. Fusion* **53**, 124037 (2011).